Sensitivity Analysis and Aerodynamic Modeling of eVTOL Low-speed Predicted Handling Qualities

Agata Rylko
PhD Candidate
Politecnico di Milano
Milan, Italy

Lorenzo Favaro
MSc Candidate
Politecnico di Milano
Milan, Italy

Giuseppe Quaranta
Full Professor
Politecnico di Milano
Milan, Italy

ABSTRACT

This study explores aerodynamic modelling and the application of Sensitivity Analysis (SA) to the low-speed predicted Handling Qualities (pHQs) of a small-scale eVTOL, to identify the impact of uncertainty in modeling. The methodology integrates the statistical simulation tool Dakota with a Flight Simulation Model (FSM) to assess the propagation of input parameter uncertainties on pHQs: Attitude Quickness, Dynamic Stability, and Bandwidth. The aerodynamic analysis, conducted using the DUST aerodynamic model, determines the correct approach for computing dynamic stability derivatives. The results highlight the dependency of these derivatives on reduced frequency, emphasizing the need to consider this in FSM development and uncertainty analysis. A hybrid SA framework that combines the Morris One-at-a-Time (MOAT) method for preliminary analysis with Variance-Based Decomposition (VBD) using a Kriging meta-model for efficiency is implemented. Key parameters whose uncertainty affects pHQs, such as mass, system time delay and aerodynamic parameters, are identified using the SA. This work demonstrates how to implement a robust SA process for uncertainty analysis, to support informed decision-making in assessing the credibility of flight simulation models to be used for certification by simulation.

NOTATION

Symbols

C_{j_0}	Zero attitude coefficient
C_{j_α}	Derivative due to angle of attack
C_{j_q}	Derivative due to pitch rate
$\mathbf{c}$	Wing chord
I_y	Moment of inertia with respect to y-axis
k	Reduced frequency
K_T	Thrust coefficient
M	Mass
q	Pitch rate
S_i	First-order sensitivity index
$S_{\mathrm{T}i}$	Total effect index
T_u	Thrust derivative due to velocity
V_{lon}	Longitudinal velocity input
μ	Mean of the Elementary Effects
μ^*	Modified Mean of the Elementary Effects
ω_n	Natural frequency
ω_{BW}	Bandwidth
σ	Standard Deviation of the Elementary Effects
τ_d	Rotor's delay
τ_p	Phase delay
θ	Pitch angle
ζ	Damping

Acronyms

ACAH	Attitude Command/Attitude Hold
EASA	European Union Aviation Safety Agency
EE	Elementary Effect
eVTOL	electric Vertical Take-off and Landing
FFT	Fast Fourier Transform
FSM	Flight Simulation Model
FTM	Flight Test Maneuver
GP	Gaussian Process
HQ	Handling Qualities
LUT	Lookup Table
MC	Monte Carlo
MHQRM	Modified Handling Qualities Rating Method
MOAT	Morris One-at-a-time
MTE	Mission Task Element
pHQ	Predicted Handling Qualities
qLPV	quasi-Linear Parameter Varying
RoCS	Rotorcraft Certification by Simulation
SA	Sensitivity Analysis
TAS	True Air Speed
TPR	Transient Peak Ratio
VBD	Variance-based Decomposition
VPM	Vortex Particle Method

Presented at the Transformative Vertical Flight 11^{th} Biennal Autonomous VTOL Technical Meeting, Phoenix, AZ, USA, Feb 4–6, 2025.

INTRODUCTION

eVTOL manufacturers are addressing new technical challenges alongside regulators and standards bodies to achieve certification. Their close collaboration is essential to ensure that new technologies, such as distributed propulsion and advanced flight control systems, meet stringent safety and performance requirements within ambitious time frames. In particular, to support compliance demonstration with EASA SC VTOL.2135 and VTOL.2145 (Ref. 1) using the EASA Modified Handling Qualities Rating Method (MHQRM) MOC.VTOL.2135 (Ref. 1) as Means of Compliance, EUROCAE released a new guideline, ED-295 (Ref. 2). The approach to collect evidence presented therein is based on newly defined Flight Test Manuevers (FTM), similar to the Mission Task Elements (MTEs) that were introduced in (Ref. 3). The MHQRM requires to investigate numerous flight conditions; some may present challenges to flight safety or be difficult to carry out these tests, or more simply the process may be too expensive to be done entirely through flight testing. Therefore, the ED-295 explicitly allows the use of simulation to complement flight tests.

To achieve the goal of applying Simulation by Certification at a desired level of decisiveness and impact, the approach outlined in the Rotorcraft Certification by Simulation (RoCS) (Ref. 4), as well as in previous publications (Ref. 5) and (Ref. 6), is followed. This approach requires first building the Flight Simulation Model (FSM) within the Domain of Validation, enabling simulation results to be compared against flight test data. During the validation process, it must be ensured that errors remain within the required tolerances, and uncertainties are assessed to evaluate the credibility of the simulation.

A similar methodology is adopted in the current research, consisting in the following steps:

1. For each FTM select a set of Predicted HQs to validate the model.
2. Identify the uncertainty associated with each relevant parameter, such as model inputs or numeric parameters.
3. Evaluate the error and uncertainty of each selected Predicted HQ metric to ensure that the error is constrained and the uncertainty is quantified.
4. Analyze the impact of simulation uncertainty on the evaluation of HQ ratings.
5. Conduct the FTM in the simulator to assess the HQ rating, taking into account the influence of uncertainty in this evaluation.

It is important to underline that the term "Predicted Handling Qualities" (pHQ) equivalent to "Flying Qualities", is intended as a set of objective characteristics of the aircraft that influence significantly the HQs, as defined in Ref. (Ref. 3). These characteristics, that can be quantified in numerical terms through a specific test, are different from the "Assigned HQ", which must instead be determined by the test pilots using the Cooper-Harper HQ rating Scale by performing specific MTEs.

In the current research, the focus is on FTM VTOL Deceleration to Hover. The chosen Predicted HQs, that is bandwidth, dynamic stability and attitude quickness in pitch, are used as fundamental indicators of the model's sufficiency for intended use, that is for flight simulation trials based on a designated FTM.

Building on the aerodynamic model developed in the previously published work (Ref. 6), which investigated the effect of propellers wake interference on the vehicle static derivatives and propeller-propeller interaction on the generated thrust, the current research addresses steps (2)-(4) of the outlined strategy. The paper begins with a sensitivity analysis aimed at quantifying the input parameters uncertainty propagation within the FSM. Based on engineering judgment, uncertainty ranges are assigned to key FSM input parameters identified as critical to the fidelity of the model. These ranges are systematically propagated through the FSM to assess their impact on the pHQ metrics. After the sensitivity analysis, the focus shifts to addressing an unresolved issue from the previous study: the dependency of dynamic stability derivatives on the reduced frequency. The derivatives are computed taking into account the variation in reduced frequency, and their resulting range of uncertainty is identified. Finally, the ranges of the identified aerodynamic parameters—dynamic derivatives from the current study and static derivatives from the previous one—are incorporated into the FSM which is utilized to recalculate the variations in pHQ metrics. This recalculation serves to verify the outcomes of the sensitivity analysis by focusing exclusively on aerodynamic parameters, providing a deeper understanding of their influence on the pHQs.

VTOL DESCRIPTION

The small unmanned eVTOL under investigation was designed and manufactured by the Aerospace Systems and Control Laboratory (ASCL) of the Department of Aerospace Science and Technology at the Politecnico di Milano (DAER) (Refs. 7–10), and is depicted in Figure 1. It utilizes 8 three-bladed propellers for vertical lift, each operating with variable RPM and fixed pitch. In helicopter mode, the aircraft is controlled by the differential thrust of all vertical propellers. For horizontal thrust, the aircraft is equipped with 2 two-blade propellers. The wings are rectangular without twist, while the empennage is H-shaped. The main geometry and mass properties of the eVTOL are detailed in Table 1. The eVTOL center of gravity is located in its vertical plane of symmetry and at 25% of the wing chord. This system has the scale of a drone and not the scale of an eVTOL capable of carrying passengers. However, it has been considered a valid benchmark for this work, since it resembles a typical lift + cruise eVTOL configuration. For the development of the FSM, it was chosen not to scale up the vehicle, to allow a direct comparison of the simulation results with future flight tests.

Table 1. eVTOL Characteristics.

Parameter	Value	Unit
Max Gross Weight	7	kg
Wing and fuselage span	3	m
Wing chord	0.26	m
Wing incidence	4.5	deg
Horizontal stabilizer span	0.721	m
Horizontal stabilizer chord	0.13	m
Horizontal stabilizer arm	1.08	m
Horizontal stabilizer incidence	0	deg
Vertical propeller diameter	0.178	m

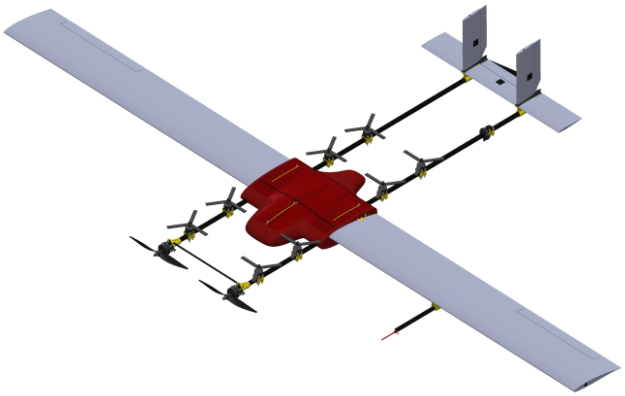

Figure 1. eVTOL overview.

METHODOLOGY AND MODELS DESCRIPTION

Sensitivity and uncertainty analysis techniques

The main features of the SA techniques employed in this work are outlined in this section. The first selected technique is Morris One-at-a-time (MOAT) which is able to distinguish between factors that have Negligible, Linear and Additive or Nonlinear/Interaction effects on the model output. The effect of each parameter, which can assume only a discrete number of values called "levels", is investigated by varying the parameter individually, along a set of "trajectories". A trajectory consists of $k+1$ points, where k is the number of specified model inputs. At each simulation point of the trajectory, only one input factor is varied with respect to the previous one (exactly "one-at-a-time"), in a derivative-like approach. In this way, for each subsequent couple of simulations, an Elementary Effect (EE) is defined as the incremental ratio produced by the changed variable. In the end, the EE distribution is averaged and two main sensitivity measures are obtained: the Mean of EE, μ, and their standard deviation, σ. A large μ is assigned to a factor whose overall effect on the output is high. In contrast, a variable with a high σ-level either undergoes nonlinear effects, increasing the variance in the results or significantly interacts with other parameters.

This work uses the Modified Mean μ^*, proposed in (Ref. 11), as an improved mean metric. μ^* averages the absolute values of the EE distribution, ranking parameters by importance and avoiding Type II errors, such as missing key parameters due to cancellation effects between EEs of opposite signs.

MOAT is primarily a method for preliminary analysis and it is not able to isolate possible interaction effects that may arise between FSM inputs from non-linearities. A more quantitative operating framework is offered by Variance-based Decomposition (VBD) approaches which, as (Ref. 12) states, help in ranking "the factors according to the amount of output variance that is removed when we learn the true value of a given input factor". To do so, a fundamental distinction shall be made between "first-order" and "total-effect" contributions. A first-order index acts as an "importance measure" of the single parameter taken alone and, for a purely additive model, represents exactly the percentage of the total output variance caused by each factor. Its quantitative representation is given by Sobol's main-effect index S_i, associated with the i^{th} input factor. When the "overall" influence on the output cannot be solely attributed to the sum of all first-order effects, an interaction between two or more variables exists. Taking this into account, for a k-dimensional model, the total variance associated with a generic output Y could then be defined as

$$V(Y) = \sum_i V_i + \sum_i \sum_{j>1} V_{ij} + \ldots + V_{12\ldots k} \tag{1}$$

as described in (Refs. 12,13), which accounts for all the possible forms of interactive effects. However the so-called "curse of dimensionality" makes "high-order" effects computation unpractical for the SA purpose. A well-established criterion is to compute the Total Effect index S_{T_i} instead, which groups the first-order effects of a factor with all of its interactive contributions. S_{T_i} not only is a standard SA index in the literature but has also shown good agreement with MOAT's μ^* and therefore allows for a comparative analysis between methods.

Since the amount of MC simulations needed to perform a VBD on the full FSM would make the process prohibitively expensive, a surrogate model is built for each of the pHQ response functions of interest, running a Monte Carlo (MC) analysis to generate a samples set of input/output relations and used to build a factor-response mapping that "emulates" the full behaviour of the eVTOL. The approach followed in this work employs Kriging interpolation (Ref. 14): building on a limited dataset of simulations performed on the true Simulink FSM, it uses the spatial correlation in the sample points to predict the value assumed by the response function at a new point, building an estimation of the unknown true response surface. This offers a fast computer emulator to be run in place of the true model to perform the MC simulations required to decompose the variance and compute Sobol Indices.

In this work, the approaches described in (Refs. 15–17) are taken as guideline. To reduce the number of FSM executions, the problem is first tackled qualitatively, performing a screening exercise through MOAT method. A VBD quantitative analysis follows, starting with a Monte Carlo simulation

set. It employs Latin Hypercube sampling strategy, which ensures a better coverage of the input space for classic random sampling strategies. Next, a Kriging metamodel is created to perform the VBD at low computational cost. Finally, MOAT results and VBD-based Sobol Indices are compared.

VTOL Flight Simulation Model description

The FSM, developed in Matlab/Simulink environment at Politecnico di Milano (Refs. 7–10), is built upon a "stitched quasi-Linear Parameter Varying" (qLPV) model. Whereas a simple LPV model is a linear system whose state-space equations show a continuous dependence on time-varying scheduling parameters, a quasi-LPV system occurs when those same scheduling parameters are also part of the states of the system, eventually resulting in non-linear feedback. When a qLPV system is coupled with non-linear equations of motion, the full model is said to be a "stitched qLPV" (Refs. 18, 19). The simulator structure is divided into two fundamental sections: an Airframe block containing VTOL's dynamics description and its integration within the external environment, and the Control Unit, further divided into fixed-wing and multicopter flight control systems.

The function of the Airframe Block is to simulate VTOL's 6DOF rigid-body dynamics by integrating its non-linear equations of motion, taking into account aerodynamic, propulsive and gravitational contributions. Regarding aerodynamics, the used model is linear, accounting for contributions from all aerodynamic coefficients and stability derivatives. Neither stall nor propeller-airframe interaction effects are accounted for by the FSM. As a consequence of the qLPV modelling approach, the aircraft's trim states are computed through interpolation of a lookup table (LUT), pre-compiled along VTOL's airspeed envelope. Similarly, aerodynamic coefficients and stability derivatives are scheduled in an airspeed-dependent LUT, . These values have been initially estimated using OpenVSP software for aerodynamic modelling. Propulsive terms computation follows an analogous path. Employing TAS information and the throttle percentage command coming from the Control Unit, vertical rotors' angular speed, thrust and torque are obtained using three-dimensional LUT, containing data obtained during experimental wind tunnel tests. After applying mixer matrix conversion, multicopter thrust and moments become available, already set in the body frame.

The Control Unit for the VTOL mode is set in a cascade control arrangement, made of four loops: body angular rates, attitude angles, inertial velocity and inertial position. While velocities and rates use full PID controllers, position and attitude rely only on proportional ones. The cascade structure proves to be particularly useful for piloting mode definition, as managing the loops, provides different levels of assistance to the pilot. To investigate pHQs , the eVTOL is always operated in Position Mode, using longitudinal and lateral inputs to control the ground speeds, V_{lon} and V_{lat} respectively, vertical inputs to control the vertical velocity V_{vert}, and a separate command for the yaw rate, expressed as yaw setpoint. Consequently, position controllers remain always disconnected throughout the pHQ simulations, except for the altitude one.

Dakota and FSM integration

A statistical simulation tool was required to adapt the existing flight simulation model for SA purposes. Thanks to its flexibility and ease of use the choice naturally fell on Dakota, a state-of-the-art software for uncertainty quantification, model calibration and optimization. It offers various variance-based/sensitivity analysis methods to be used in Design of Computer Experiments practice, parameters studies, together with meta-modeling capabilities for the construction of powerful surrogate models. Moreover, it can be easily coupled with external computational codes such as the eVTOL FSM, by means of text files, treating the physics-based simulation models as simple black-boxes. More about Dakota, sensitivity and uncertainty analysis capabilities can be found in the related manual and software training documents (Refs. 14, 20–22).

DUST Aerodynamic model description

As a more accurate aerodynamic modelling approach, the computational tool called DUST developed by Politecnico di Milano, was used. DUST is open-source software that allows for the modelling of solid bodies such as thick surface panels, thin vortex lattice elements, and lifting line elements. In this study DUST version with the reformulated Vortex Particle Method (VPM) was used, which provides a more realistic wake modeling, through the reformulated vortex stretching estimation, described in (Ref. 23). The model developed in (Ref. 6) was used in configuration without the propellers, composed of wing and horizontal stabilizer. For the fixed lifting surfaces, vortex lattice elements were used, without aerodynamic tables correction (inviscid flow).

Dynamic stability derivatives due to pitch rate, C_{L_q} and C_{Mm_q} were calculated based on the single point method outlined in (Refs. 24, 25), by imposing a sinusoidal oscillatory pitching motion to the eVTOL. According to this method, the dynamic stability derivative, expressed as a coefficient dependent on the angle of attack, can be expressed as follows:

$$c_{jq} = \frac{\Delta c_{jq}(t)|_{t=t_{\alpha_0}}}{\alpha_A k} \tag{2}$$

where α_A is the amplitude of the angle of attack for pitching oscillation, k is the reduced frequency, and the term $\Delta c_{jq}(t)|_{t=t_{\alpha_0}}$ corresponds to the operation of measurement of the thickness of the aerodynamic force or moment hysteresis ellipse around α_0 (see Figure 2).

SENSITIVITY ANALYSIS RESULTS AND DISCUSSION

To approach the pHQ definition problem systematically, the previously described SA techniques are merged together into

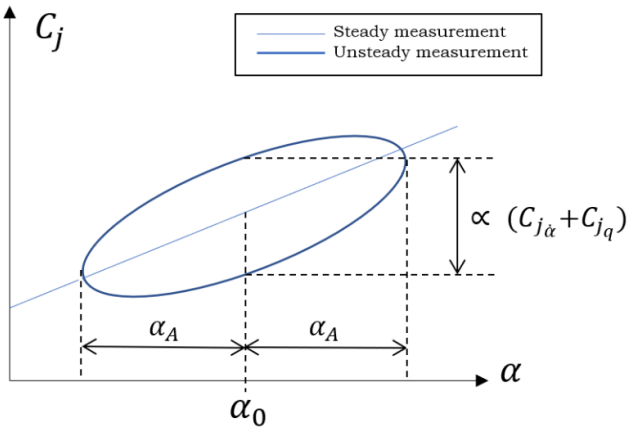

Figure 2. Graphical representation of the extraction of the dynamic derivative, from (Ref. 24).

a unique, comprehensive simulation framework. This allows for the repeatability of the tasks and makes the results on different pHQs comparable.

Table 2 shows the main FSM factors to whom an uncertainty range has been assigned, which are composed of three main subgroups: eVTOL's mass and inertia parameters (namely M and the pitch inertia moment I_y), aerodynamic coefficients and stability derivatives related to the longitudinal dynamics, and vertical rotors' characteristics. The latter include rotors' thrust coefficient K_T, thrust's dependence upon the longitudinal speed (modeled as a gain on the airspeed information fed by the FSM Sensor Unit to the thrust-related LUT, as not to influence thrust dependence upon throttle command) and an artificially added delay in rotors' response, formulated as a simple time-delay. The reason behind its addition comes from a series of experimental tests (Ref. 9) that indeed highlighted a significant delay A small amount of delay (0.02 s) was manually inserted in the system, allowing for the characterization of its effect on eVTOL's dynamic behaviour. It should be noted that the parameters list was originally longer, including parameters possibly related to the coupling between the pitch and the roll axes . However, a SA factor screening based on ADS-33 3.3.9.2 requirement ("Roll-due-to-pitch Coupling for Aggressive Agility") showed that there was no significant inter-axes coupling and all roll-related factors were consequently discarded.

Due to the differing nature of the factors, uncertain ranges are assigned based on different logic: aerodynamic and stability terms are derived from their nominal values, with a 20% increase/decrease applied. Similarly, I_y, K_T and T_u are defined in percentage terms, limiting their range of variability to avoid excessive interference with pHQ-related manoeuvres. The rotor delay, τ_d, as previously stated, follows the same logic. Since "there is insufficient information concerning the quantity of interest to specify either a fixed value or a precisely known probability distribution" (Ref. 26), all of these factors are treated as epistemic uncertain parameters, with their distributions generically assumed to be uniform. The mass has been varied in both directions by a maximum of 0.5 kg, accounting for the possibility of missions with different payloads; again, a uniform distribution has been used.

Table 2. SA uncertain input variables.

Parameter	Value	Range	Unit
M	7	$\pm$ 0.5	kg
I_y	0.7237	$\pm$ 10%	kg $\cdot$ m^2
K_T	$6.96 \cdot 10^{-8}$	$\pm$ 15%	-
T_u	1	$\pm$ 5%	-
τ_d	0	+ 0.03	s
C_{L_0}	0.7745	$\pm$ 20%	-
C_{D_0}	0.0183	$\pm$ 20%	-
$C_{M_{m_0}}$	-0.0240	$\pm$ 20%	-
C_{L_α}	5.1270	$\pm$ 20%	-
C_{D_α}	0.2558	$\pm$ 20%	-
$C_{M_{m_\alpha}}$	-0.5402	$\pm$ 20%	-
C_{L_q}	7.6136	$\pm$ 20%	-
C_{D_q}	0.7179	$\pm$ 20%	-
$C_{M_{m_q}}$	-16.169	$\pm$ 20%	-

In the following paragraphs, a brief description of the required test manoeuvres and of the main adopted metrics precedes the SA results.

Moderate-amplitude pitch Attitude Changes (Attitude Quickness)

The first pHQ to be analyzed refers to ADS-33 Requirement 3.3.3, Pitch Attitude Quickness: the idea behind this criterion is "to characterize the helicopter's ability to achieve rapid, precise attitude changes when performing sharp, moderate amplitude manoeuvres" (Ref. 27).

However, given the dynamics and control system architecture of the eVTOL under study, a re-interpretation of the requirement was needed, for two main reasons. The first one regards the input specification: ADS-33 suggests the application of a step in the longitudinal cyclic for ACAH Response Types or a pulse for Rate Response Types. In the case of the eVTOL, when operated in Position Piloting Mode, this translates into a ΔV_{lon} input, thus making the identification of the Response Type challenging, not being directly linked to either of the previous categories. However, given that when a positive control input in the longitudinal speed is applied to the FSM, the drone pitches down to achieve the α_{trim} required by the new condition and when the command is released, the eVTOL returns to its previous state, in a fashion similar to what an ACAH-flown helicopter would do, a step was chosen as the best input option to perform the test.

The second challenge is associated with the correct definition of the output metrics: ADS-33 asks for the attitude change to "be made as rapidly as possible from one steady attitude to another" (Ref. 3) and requires the extraction of two quantities from the outputs' time histories: the ratio of the peak angular rate reached after application of the step to the peak θ change and the minimum attitude excursion experienced by the vehicle before reaching the new steady attitude. In the case

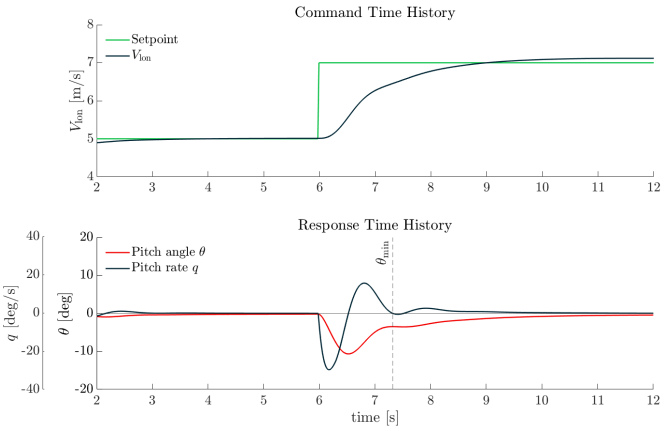

Figure 3. Attitude Quickness, Test Manoeuvre.

of this study the latter measure, mainly due to the small trim pitch angle the eVTOL flies at, does not directly fit the definition provided by ADS-33: in fact, when a step is applied to the FSM after its maximum attitude change the vehicle finds a new trim state without any undershoot, not allowing for a clear $\Delta\theta_{\text{min}}$ to be measured. The problem is overcome by looking at the recorded pitch-rate time history: the minimum attitude change is then taken as the angle reached by the vehicle when the on-axis angular rate approaches a stationary point for the second time after the application of the controller input.

Figure 3 shows the input/output time histories: ΔV_{lon} has been chosen as not to undergo stall effects (over all of the SA simulations $\Delta\theta_{\text{pk}}$ does not exceed 13 deg); this brings with it a limitation on the $\Delta\theta_{\text{min}}$, which indeed always remains below required minimum attitude change of 5 deg . Nevertheless, this does not affect the SA, which is still able to highlight the main trends.

Figures 4 and 5 display the Modified Mean μ^* against the standard deviation σ of the computed Elementary Effects, as in (Ref. 16). The parameters located in the lower right-hand area behave mostly monotonically, if not almost linearly, and appear to be highly significant in driving model's behaviour, but without interactions with the other uncertain variables. On the other hand, the variables placed in the upper left-hand region show a high non-linear/interactions effect. The x-axis representation quantitatively captures the outputs' variability. . Since μ^* is derived from the absolute value of the mean of the Elementary Effect (EE), it also indicates how much the output varies, on average, when varying the corresponding input of one Δ level. To compare factors and assess the relative importance, the criterion based on μ^* is selected. Alternatively, the Euclidean distance from the origin in the $\mu^* - \sigma$ plane could be employed (Ref. 15).

Figure 4 shows the results of MOAT application to $\Delta\theta_{\text{min}}$ index: at first glance, it is immediately clear that almost all factors behave monotonically, with little or no non-linearities/interactions. Secondly, a large number of them seem to affect the output measure, from mass to aerodynamic parameters. Aerodynamics plays indeed a role of primary importance: all lift-related coefficients are present, with a pre-

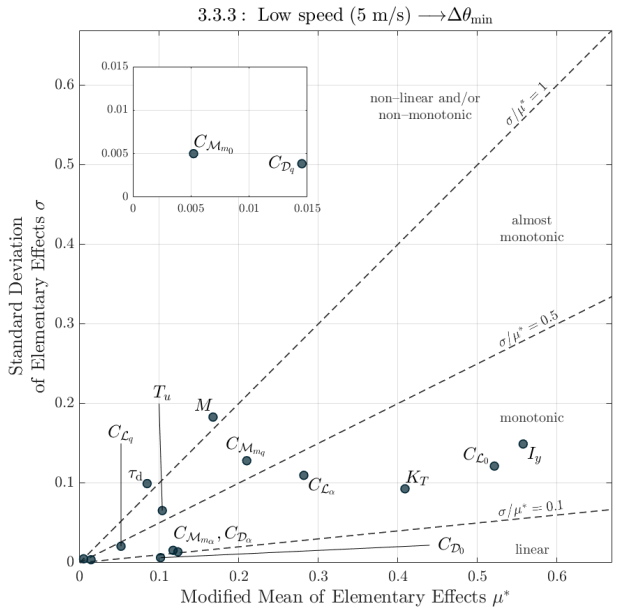

Figure 4. Attitude Quickness, $\Delta\theta_{\text{min}}$ Results.

dominance of C_{L_0} and C_{L_α}. Pitching-moment stability derivatives appear too, together with drag-related ones (this constitutes a unicum among all the performed analyses, as pHQ rarely show dependence on drag, as emerges from the following paragraphs). Among the others, I_y and K_T prevail.

Figure 5 illustrates how the behaviour changes drastically when focusing on the quickness metrics, making the distinction between parameters clearer. The eVTOL is mainly guided by mass and rotor-related factors, with response delay τ_{d} assuming a bigger role. As for aerodynamics, only C_{L_0} and C_{L_α} are visible. The other parameters are relegated to smaller orders of magnitude.

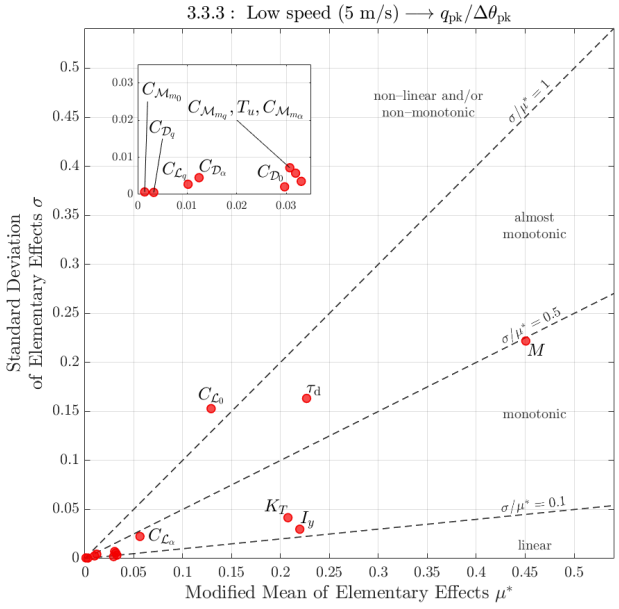

Figure 5. Attitude Quickness, $q_{\text{pk}}/\Delta\theta_{\text{pk}}$ Results.

MOAT results are now complemented with Kriging ones. Firstly a 500-sample MC simulation is performed, from which Dakota builds two different GP surrogates, one for each pHQ sensitivity measure. The metamodel is hence available to apply a VBD technique, from which Sobol indices are computed. The results are divided into two subsets: the S_i related to the first-order effects and the overall S_{T_i} related to the Total Effects, thus dividing each factor's own effect from its interaction with the others.

In Figure 6 Sobol Indices for both pHQ metrics are shown. Focusing on the minimum attitude change, good agreement with MOAT results is visible: both methods identify I_y, K_T and aerodynamic terms as the most significant ones, confirming the utmost importance of C_{L_0}, C_{L_α} and $C_{M_{m_q}}$. The small cluster of C_{D_0}, C_{D_α} and $C_{M_{m_\alpha}}$ is also correctly identified by both methods, with some small differences in the $\mu^* - S_{T_i}$ ranking as the variable importance decreases. Even though most of the variance is explained by the Main Effects, M and τ_d mainly contribute to the output through higher-order terms. This can be ascribed to their interactive effect: this can be ascribed to the lower end of the mass uncertainty range that, when combined with a sufficiently high level of rotors' delay, eventually drives the system into a sustained oscillation, hence causing a high level of variance in the results. The same combined effect reflects also into the pHQ specification of Figure 7: some outliers are in fact produced in the upper part of the MC output distribution, in both $\Delta\theta_{min}$ and $q_{pk}/\Delta\theta_{pk}$, which arise when both the mass and the delay simultaneously reach the extremes of their prescribed ranges.

Regarding the quickness index, VBD confirms MOAT results for the first 5 input factors (mass parameters, rotors' features and C_{L_0}). Although both methods correctly identify C_{L_α}, T_u and $C_{M_{m_\alpha}}$, some discrepancies affect the lower-end part of the ranking, as $C_{M_{m_0}}$ and C_{D_q} gain some positions with respect to the previous MOAT results, especially thanks to higher order effects (as shown by the white-coloured part of the histogram): even if these parameters are of much smaller of importance for the others (both MOAT and VBD locate them at a lower order of magnitude) and do not influence the factor prioritization process significantly, some caution should be placed in considering the effects of the aerodynamic parameters.

Figure 7 projects the MC results on the ADS-33 requirement plane: most of the variability is visibly displaced along the y-axis with the quickness values ranging from 2.5 to 3.25 ($\pm$13%). Furthermore, they exceed the typical limits the document prescribes for helicopters, being way above the Level 1 threshold which is due to the small dimensions of the vehicle.

Mid-term Response to Pitch Control Inputs (Dynamic Stability)

In this section, Requirement 3.3.2.3 is analyzed: the pHQ refers to the vehicle's dynamic stability and investigates eVTOL's poles, as extracted from the pitch-rate free response to a pulse in the longitudinal controller. In Figure 8 the main time

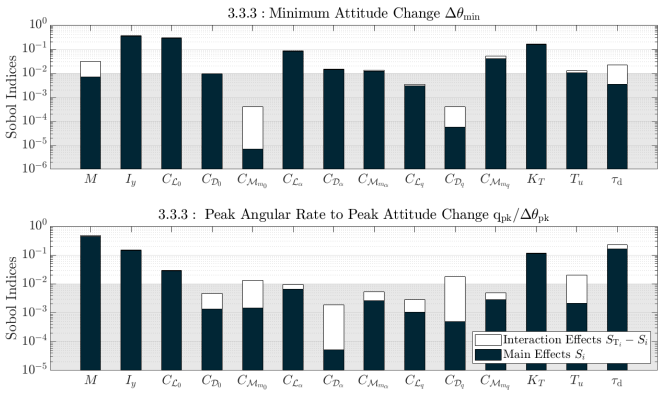

Figure 6. Attitude Quickness, VBD Results.

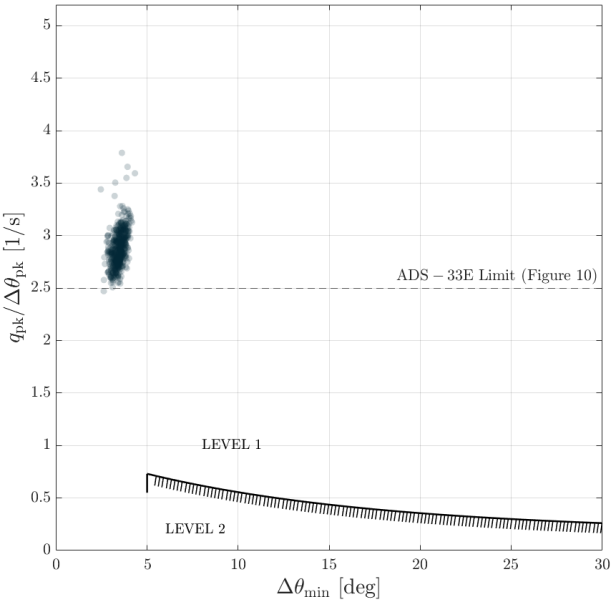

[1] The applied levels are derived from helicopter standards and may require revision to align with eVTOL-specific characteristics.

Figure 7. Attitude Quickness, pHQ ADS-33 Results.[1]

histories requirements are shown. Since ADS-33 states that "the portion of the time history used to calculate the damping ratio should occur after the input is completed", the first oscillation - driven by the pulse in the longitudinal speed - is neglected. Furthermore, it is important to measure the damping ratio from the free response only, not the forced response: this raised some concerns about the effect of the onboard attitude and rate controllers, which rapidly take the aircraft back to the previous trim state. To limit the effect of the control system on the response, the damping ratio ζ has been measured - using the Transient Peak Ratio (TPR) criterion, as suggested by ADS-33 itself (Ref. 3), employing the first peak and the first valley only. The second positive peak has been used only as a mean to compute the characteristic period of the oscillation and its natural frequency ω_n.

The MOAT results exhibit two main trends: first of all, aerodynamics assumes greater importance than in the Quickness framework, as C_{L_0} and $C_{M_{m_q}}$ figure among the factors with the highest μ^* for the damping ratio ζ, to which C_{L_q}, C_{D_α} and

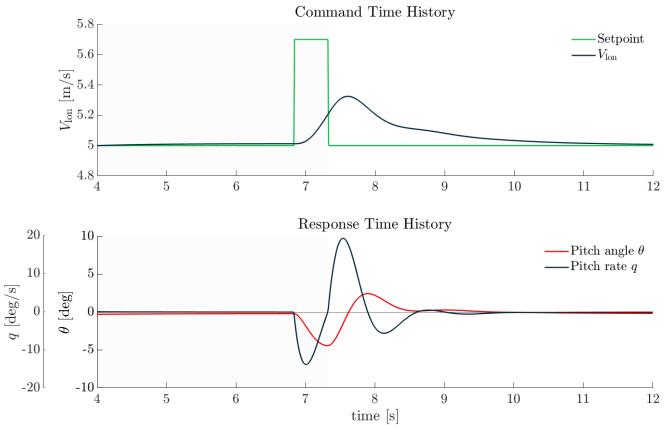

Figure 8. Dynamic Stability, Test Manoeuvre.

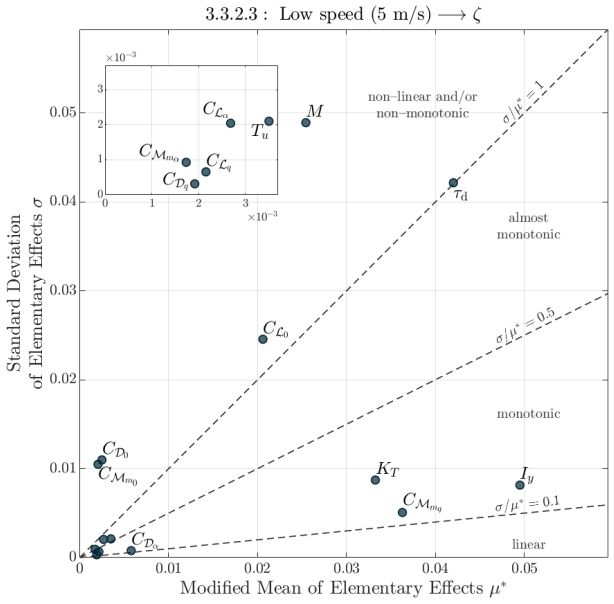

Figure 9. Dynamic Stability, ζ Results.

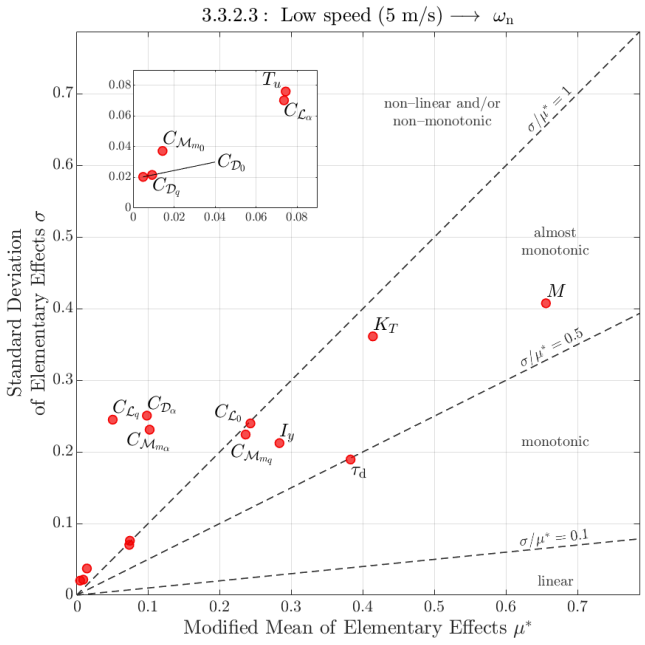

Figure 10. Dynamic Stability, ω_{n} Results.

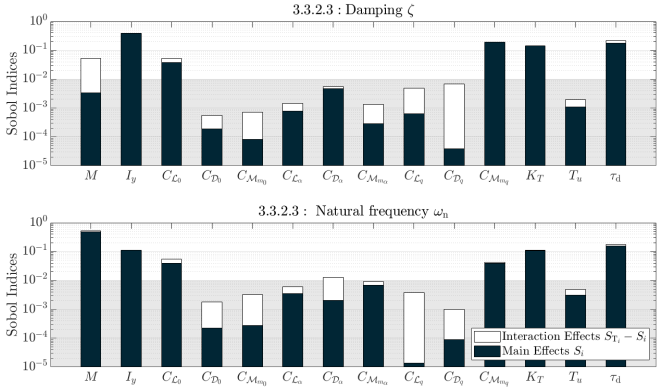

Figure 11. Dynamic Stability, VBD Results.

$C_{M_{m\alpha}}$ are added for the natural frequency. The second one is the high level of standard deviation associated with M and τ_{d} in the ζ results: this may suggest the existence of non-linearities or, possibly, an interactive effect between the variables (Figures 9 and 10).

Sobol Indices in Figure 11 confirms the MOAT results and, as the MOAT itself already predicted, indicate a strong Total order effect coming from the mass factor. Analyzing the MC training set, a behaviour analogous to the one described for the minimum attitude change in the previous section was recognized: when combined, mass and rotors' delay eventually drive the system into a Level 2 ζ specification.

Figure 12 shows how the aircraft flies over the Level 1/2 margin, with a predominance of Level 1 simulations. As MOAT highlighted in Figures 9 and 10, while the damping oscillates around the $\zeta = 0.35$ line of about ± 0.5, the frequency has a much wider variability and furthermore is much higher than the typical helicopter values expected by ADS-33 (far from the axes origin).

It is important to note that the DS values for this vehicle shown in Figure 12 lie well above the typical scale of the ADS-33 graph, with $\omega_n = 5.61$ rad/s corresponding to a natural oscillation frequency of 0.9 Hz. This represents a very high frequency, attributed to the small size of the vehicle.

Short-term Response to Pitch Control Inputs (Bandwidth)

The last pHQ subjected to analysis is 3.3.2.1, referred to as Bandwidth, which investigates aircraft's behaviour in the frequency domain, over a frequency range of interest. The reasoning behind the application of this requirement is "to determine if there is sufficient phase margin to allow the pilot to close the attitude loop [...] without threatening stability" (Ref. 28). The test course requires the pilot to apply a frequency sweep input in the longitudinal controller and to register the pitch angular rate response, which are processed by means of a Fast Fourier Transform (FFT) to obtain Bode plots. The two quantities of interest are ω_{BW} (bandwidth) - taken as

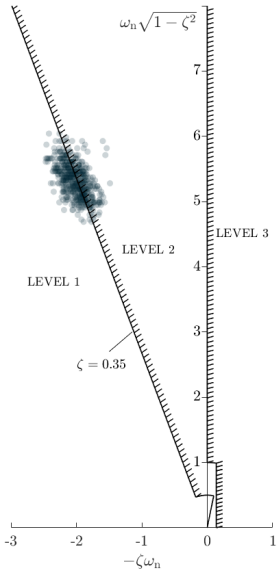

[2] The applied levels are derived from helicopter standards and may require revision to align with eVTOL-specific characteristics.

Figure 12. Dynamic Stability, pHQ ADS-33 Results.[2]

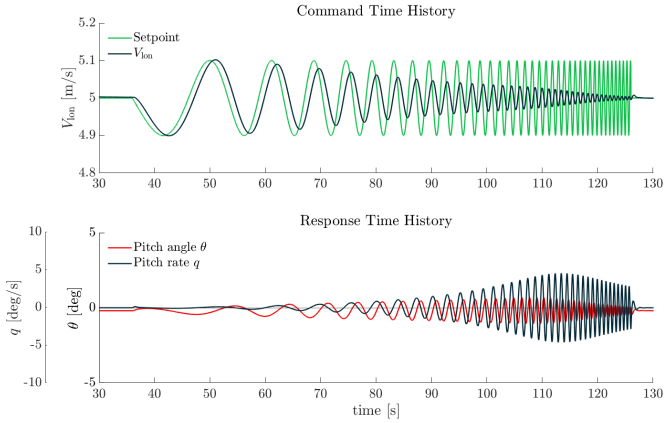

Figure 13. Bandwidth, Test Manoeuvre.

$\omega_{BW_{\text{phase}}}$ because of the ACAH Response Type (Ref. 3) - and τ_p (phase delay).

Following the instructions of (Ref. 28), a 90 s long automated sweep is generated , with a frequency content linearly increasing from 0.3 rad/s to 12 rad/s (approximately from 0.05 Hz to 2 Hz) that is the pilot frequency of interest. Figure 13 illustrates the reference sweep in the longitudinal speed (green curve) and the related q-rate response.

However, setting a 90 s input naturally leads to inherently time-demanding simulations which, in the context of a MOAT or MC analysis, could easily become prohibitively expensive. To overcome this problem, a different approach is explored for the purposes of SA application. Instead of analyzing the full non-linear system response, the criterion is instead applied to a linearized FSM . The main idea is to linearize the longitudinal dynamics near a trim condition point and to generate the related Bode plot employing Matlab®/Simulink® *Model Linearizer* routine. By doing so, the time cost is significantly brought down and the main trends in eVTOL's bandwidth behaviour are still captured. To check for the applicability of the method, FFT-based response of the full non-linear system is compared to the linearized one (around a $V_{\text{lon}} = 5$ m/s trim point), as shown in Figure 14 .

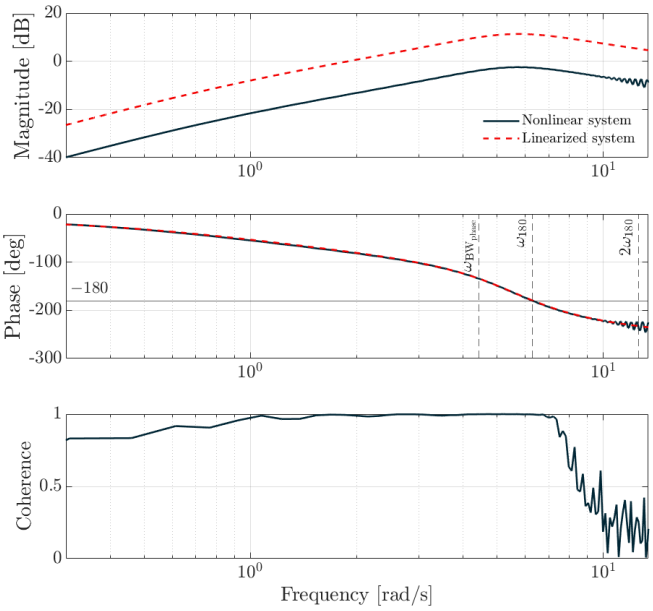

Figure 14. Closed-loop Bode plot for $q/\Delta V_{\text{lon}}$.

Even though some discrepancies are present between the magnitude Bode plots, the phase behavior shows to be valid inside of the specified frequency range. It should be made clear that the agreement between models holds as long as the sweep applied to the non-linear model stays within reasonably small amplitudes. As the applied sweep's amplitude increases, differences may arise. A coherence plot is also shown for the FFT-based results, as ADS-33 indicates a minimum value of 0.6 to check for the goodness of the non-linear system sweep results.

The discussion of Bandwidth SA results is straightforward, following the main considerations already made for the previous pHQ. In both SA indices (from Figures 15 and 16) - aside from the typical prevalence of the mass, inertia and thrust coefficient - aerodynamics exhibits a noticeable effect, mainly due to C_{L_0} and $C_{M_{m_q}}$. At a lower level, at least for the bandwidth metrics, α-related derivatives must be also accounted for. Sobol Indices confirm the MOAT results , as shown in Figure 17.

At last, the MC results are compared with the expected limits: Figure 18 shows a cluster of points well above the threshold between the levels, placing the eVTOL in Level 1. $\omega_{BW_{\text{phase}}}$ shows a wider range of variability for τ_p: when parameters are varied in the MOAT and MC simulations the Bode phase curve undergoes greater variation in the range between the bandwidth and the crossover frequency (ω_{180}), shifting bandwidth values all over the 4-5 rad/s interval. Since the phase curve is less sensitive to variations for $\omega > \omega_{180}$, τ_p instead remains almost unchanged after ω_{180}, resulting in a much lower variance in phase delay results.

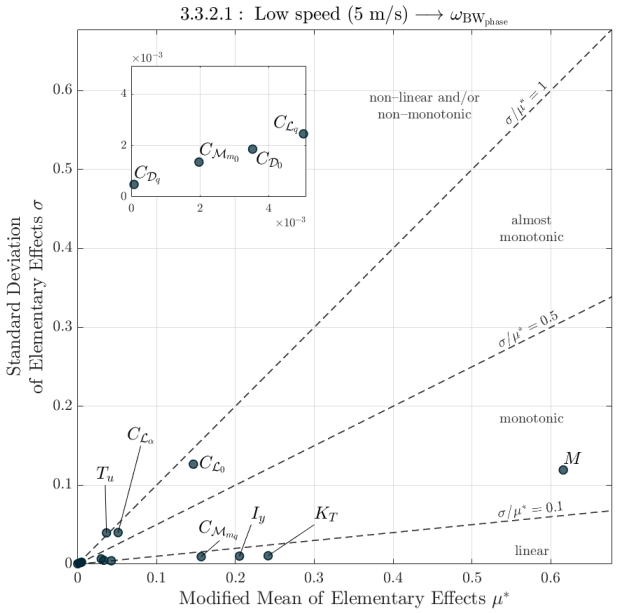

Figure 15. Bandwidth, $\omega_{BW_{phase}}$ Results.

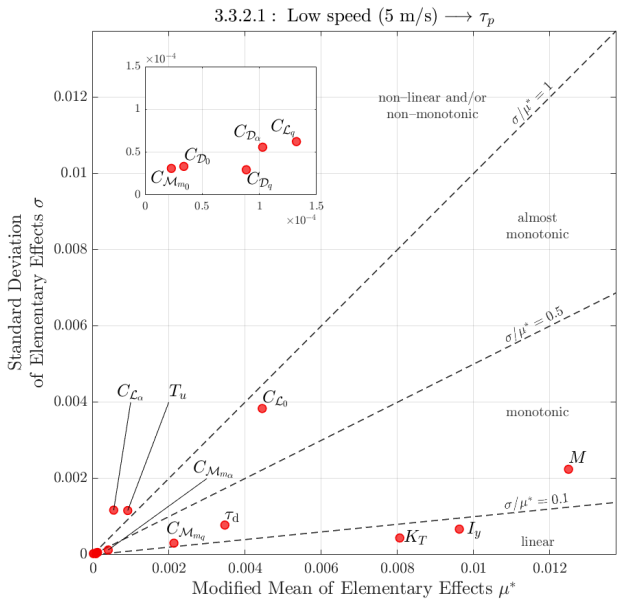

Figure 16. Bandwidth, τ_p Results.

AERODYNAMIC ANALYSIS RESULTS AND DISCUSSION

Dynamic stability derivatives for an isolated wing based on the Theodorsen model

In the previous work (Ref. 6), the derivatives due to pitch rate C_{L_q} and C_{Mm_q}, computed according to the methodology reported in (Refs. 24, 25) were found to be dependent on the oscillation frequency. To understand this unexpected dependency, a comparative study with a simple isolated rectangular wing, using Theodorsen theory was conducted. The eVTOL wing has a relatively high aspect ratio $b/c = 11.5$, so the 3D flow effects have less influence on the unsteady aerodynamics and Theodorsen's theory can provide a useful approximation of the aerodynamic response. A detailed description of the model and the derivation of the equations can be found in (Ref. 29). The methodology allows to compute the static and dynamic derivatives for pitching and plunging sinusoidal oscillations, to evaluate their dependency on frequency. In this section only the dynamic derivatives are reported, computed as follows, for the pitching oscillation $\alpha = \alpha_0 sin(\omega t)$:

$$C_{L_q} + C_{L_{\dot{\alpha}}} = \frac{1}{k}\frac{\Im(\mathsf{C_L})}{\alpha_0} \tag{3}$$

And for the heave oscillation $h = h_0 sin(\omega t)$:

$$C_{L_{\dot{\alpha}}} = -\frac{1}{k^2}\Re(\mathsf{C_L})\frac{c}{2h_0} \tag{4}$$

Where k is the reduced frequency $k = \frac{c\omega}{2U_\infty}$.

Figure 19 presents the results obtained for different pitching and heave oscillation frequencies, in function of reduced frequency, which range corresponds to frequencies between 0.1 and 3 Hz. The calculations were performed for a wing with

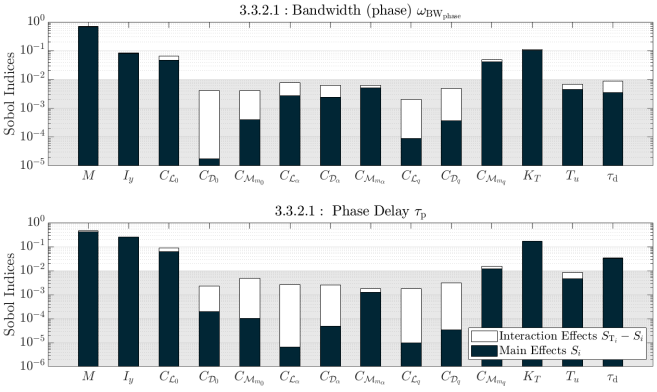

Figure 17. Bandwidth, VBD Results.

a non-symmetric profile Selig 2046, for incompressible and inviscid flow, in the range of $\alpha = \pm 5$ deg. The amplitude of sinusoidal pitching motion was set to 2 deg for all simulations. The heave amplitude was imposed so that the resulting amplitude of the angle of attack oscillation was equal to 2 deg.

The lift dynamic derivative, $C_{L_q} + C_{L_{\dot{\alpha}}}$, exhibits a strong dependency on the reduced frequency, which becomes less pronounced at higher reduced frequencies. The lift dynamic derivative due to heave motion, $C_{L_{\dot{\alpha}}}$, shows a similar dependency on the reduced frequency, is always negative, and cannot be neglected. The lift derivative due to pure pitch rate, C_{L_q}, was determined as the difference between the aforementioned quantities and corresponds to a value that could be obtained by simulating a phugoid motion where $\alpha = \text{const}$. It is positive, indicating that an increase in pitch rate (nose-up motion) results in an increase in overall lift and it decreases at higher reduced frequencies, due to the growing influence of unsteady flow effects.

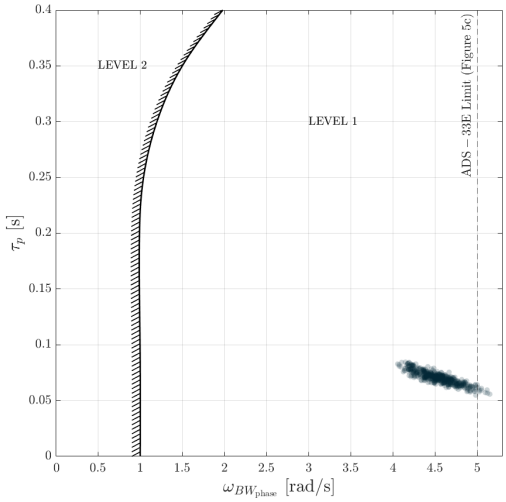

[3] The applied levels are derived from helicopter standards and may require revision to align with eVTOL-specific characteristics.

Figure 18. Bandwidth, pHQ ADS-33 Results.[3]

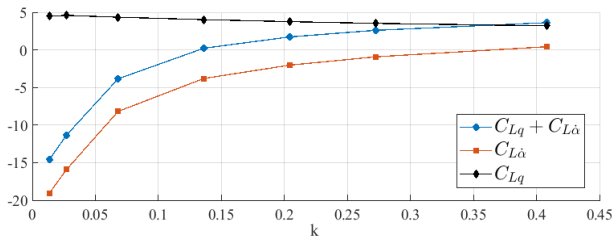

Figure 19. Lift derivative due to pitch rate vs reduced frequency, for pitch oscillation and pure heave case, obtained based on Theodorsen theory.

Stability derivatives results using DUST model

In this section, the results of the calculation of lift and pitching moment derivatives in DUST are reported. Figure 20 shows the lift and pitching moment dynamic derivatives, $C_{L_q} + C_{L_{\dot{\alpha}}}$ and $C_{Mm_q} + C_{Mm_{\dot{\alpha}}}$ respectively, for an isolated wing, obtained from pitching sinusoidal oscillations conducted using DUST. It can be seen that the lift dynamic derivative has the same dependency on the frequency as in Figure 19 and is positive. The pitching moment dynamic derivative is negative, meaning that the wing is self-stabilizing.

Both methods exhibit similar trends in the computation of the dynamic stability derivatives, but there still are quantitative differences in the magnitude of derivatives. Figure 21 represents the lift and pitching moment dynamic derivatives, for a wing and horizontal tail. It was obtained by oscillation of 2 deg about a 0 mean angle of attack. It can be seen that the horizontal tail provides a negative contribution to the pitching moment derivative due to pitch rate. A negative C_{Mm_q} is essential for longitudinal dynamic stability, as it ensures the damping of oscillatory modes like the short-period mode or phugoid mode. As expected, for different velocities, but maintaining the same k, the computed derivatives have the same values.

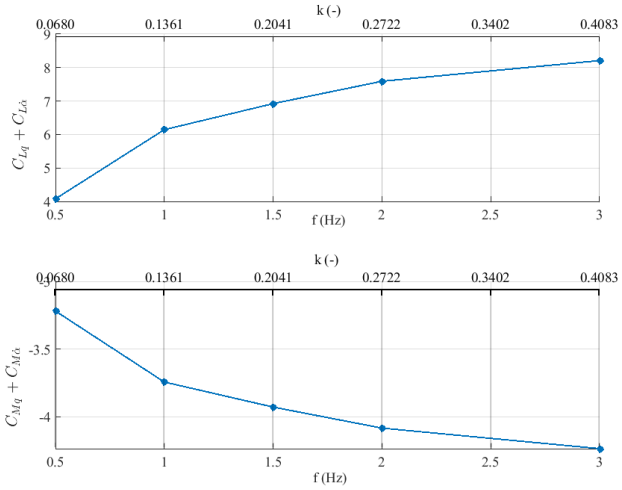

Figure 20. Lift and pitching dynamic derivatives for an isolated wing, for 6 m/s.

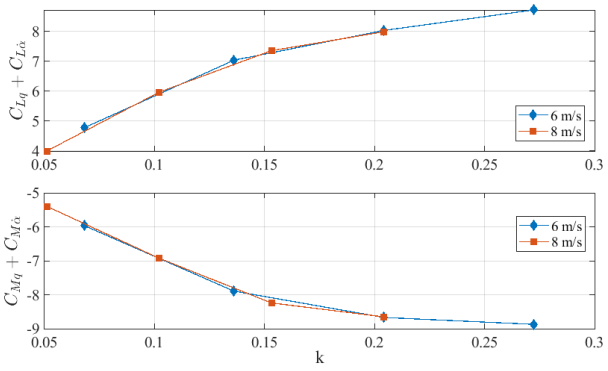

Figure 21. Lift and pitching dynamic derivatives for a wing and horizontal stabilizer, for 6 and 8 m/s.

Moderate-amplitude pitch Attitude Changes (Attitude Quickness)

Based on the MOAT and VBD results presented in the previous section, significant aerodynamic parameters were selected to perform comparative Attitude Quickness simulations (see Table 3). The initial ranges of aerodynamic parameters, as listed in Table 2, were refined by studying the influence of propeller wake on the static stability derivatives and the effect of viscosity on the computation of C_{L_α} (Ref. 6), as well as the variation in dynamic derivatives due to frequency, as discussed in the previous subsection.

The maximum value of C_{L_0} represents the value without propeller wake interference, while the minimum value accounts for lift loss on the wing and negative lift on the horizontal stabilizer. Although C_{Mm_0} would also change due to propeller wake interference, it is kept constant in this study, as it was found to be negligible in the previous sensitivity analysis. The minimum value of C_{L_α} corresponds to the lift coefficient of the wing and horizontal tail for inviscid flow, while the maximum value was computed in (Ref. 6), considering low Reynolds numbers for the vehicle scale and flight velocity. The maximum and minimum values of C_{L_q} and C_{Mm_q} were computed

Table 3. Aerodynamic parameters values for Attitude Quickness.

Case:	1	2	3	4	5
C_{L_0}	0.4524	**0.6268**	**0.6268**	**0.6268**	**0.6268**
$C_{M_{m_0}}$	-0.0240	-0.0240	-0.0240	-0.0240	-0.0240
C_{L_α}	5.115	5.115	**7.48**	**7.48**	**7.48**
$C_{M_{m\alpha}}$	-0.5402	-0.5402	-0.5402	-0.5402	-0.5402
C_{L_q}	5.9649	5.9649	5.9649	**7.9898**	**7.9898**
$C_{M_{mq}}$	-6.9263	-6.9263	-6.9263	-6.9263	**-8.6516**

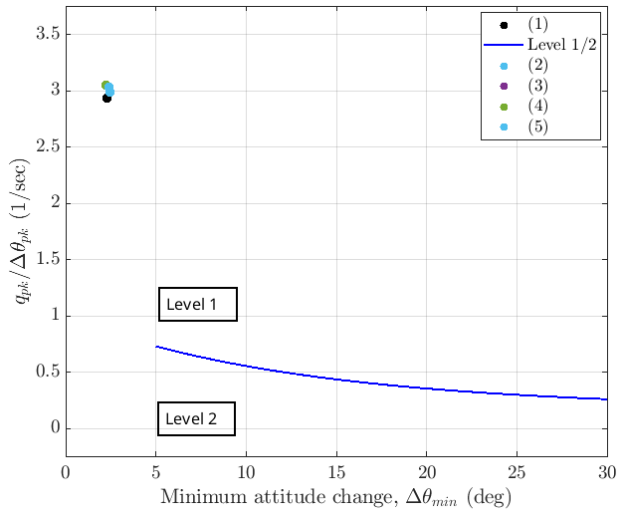

[1] The applied levels are derived from helicopter standards and may require revision to align with eVTOL-specific characteristics.

Figure 22. Attitude Quickness results variability due to uncertainty of aerodynamic parameters.[1]

Table 4. Aerodynamic parameters values for Dynamic Stability.

Case:	1	2	3	4
C_{L_0}	0.4524	**0.6268**	**0.6268**	**0.6268**
$C_{M_{m_0}}$	-0.0240	-0.0240	-0.0240	-0.0240
C_{L_α}	5.115	5.115	5.115	5.115
$C_{M_{m\alpha}}$	-0.5402	-0.5402	-0.5402	-0.5402
C_{L_q}	5.9649	5.9649	5.9649	5.9649
$C_{M_{mq}}$	-6.9263	-6.9263	**-8.6516**	**-16.169**

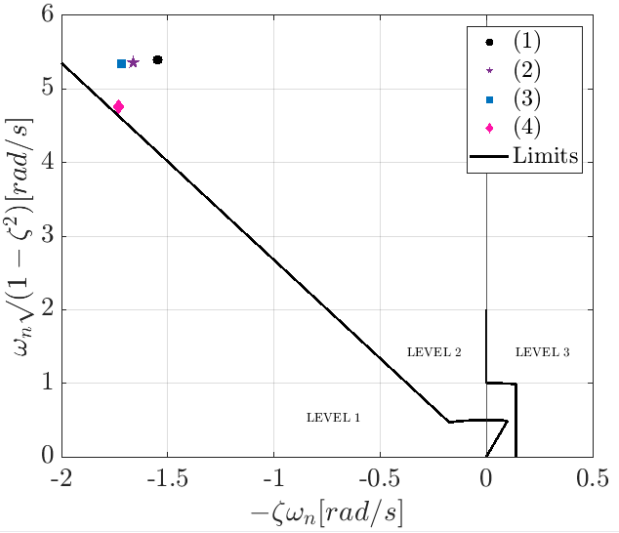

[1] The applied levels are derived from helicopter standards and may require revision to align with eVTOL-specific characteristics.

Figure 23. Dynamic Stability variability due to uncertainty of aerodynamic parameters.[1]

for $k = 0.1$ and $k = 0.2$, respectively, corresponding to oscillation frequencies of $0.7 - 1.5$ Hz.

The manoeuvres were conducted in the same manner, with an initial trim condition in forward horizontal flight at 5 m/s, giving a step input into the horizontal velocity V_{lon}. The results of Attitude Quickness are presented in Figure 22. No delay was introduced ($\tau_d = 0$). The changes to the aerodynamic parameters were implemented gradually, one parameter at a time, in each simulation.

As anticipated in SA, this analysis confirms that the attitude quickness parameter exhibits low sensitivity to variability in aerodynamic parameters. Even when these parameters are modified, the quickness value at the uppermost position on the y-axis is only 4% higher than the baseline value, indicating a limited influence. The variability in the minimum attitude change further reinforces this observation. Despite simultaneous changes to multiple aerodynamic parameters, the variability is constrained within a narrow range, spanning from -4% to $+7\%$.

This consistency implies that the aerodynamic parameters exert only a marginal effect on attitude quickness, at the investigated low speed and small amplitudes, and are predominantly governed by other factors, such as mass or delay, or are inherently robust to aerodynamic variability. This behaviour might change at higher speeds and higher pitch angles, where dynamic stall effects should be considered.

Mid-term Response to Pitch Control Inputs (Dynamic Stability)

Following the strategy outlined in the previous subsection, the most significant aerodynamic parameters for Dynamic Stability, identified from the SA analysis—namely C_{Mmq} and C_{L_0}—were selected to perform a quantitative comparison of Dynamic Stability results (see Table 4). Again, the simulations were performed in the same way, introducing a pulse of $V_N = 0.7$ m/s of duration of 0.5 s during a trimmed horizontal flight at 5 m/s. The damping and natural frequency were computed, as described in the previous section dedicated to Dynamic Stability, considering the first peak and the first valley of pitch rate for ζ, and including the second positive oscillation peak for ω_n.

In contrast to Attitude Quickness, Dynamic Stability demonstrates greater sensitivity to aerodynamic parameters (see Figure 23), such as C_{L_0} and $C_{M_{mq}}$. The lift coefficient C_{L_0} visibly influences damping, particularly shifting the pHQ closer to Level 1 under the studied conditions. This indicates that ignoring the effects of propeller wake interference, which

decreases the zero aerodynamic lift coefficients, can lead to overestimated stability predictions. Moreover, as previously stated, the small vehicle's dimensions result in higher and more spread ω_n values, which exceed typical helicopter scales.

After computing the dynamic derivatives in this subsection, it was observed that the obtained C_{Mmq} is significantly higher than the values reported in recent studies (Refs. 7–10). This value was also used in the sensitivity analysis conducted in the previous section (see Table 2). Due to the high sensitivity of the DS to C_{Mmq}, a comparative simulation, referred to as (4) in Table 4, was performed, which demonstrates further increment in ζ and a decrease in ω_n. The discrepancies between the results could not be explained, either by tracing back the design changes of the aircraft or by analyzing the employed reference frames.

Short-term Response to Pitch Control Inputs (Bandwidth)

The bandwidth and phase delay trials described in this section were conducted using the non-linear FSM, and with a greater sweep amplitude compared to the simulations presented in the sensitivity analysis section. The sweep was performed with an amplitude of $V_{lon} = 0.5$ m/s, resulting in a maximum pitch angle of approximately 5°. It was verified that this amplitude does not affect the computation of bandwidth and phase delay.

Table 5. Aerodynamic parameters values for Bandwidth and phase delay.

Case:	1	2	3	4	5
C_{L_0}	0.4524	**0.6268**	**0.6268**	**0.6268**	0.4524
$C_{M_{m_0}}$	-0.0240	-0.0240	-0.0240	-0.0240	-0.0240
C_{L_α}	5.115	5.115	**7.48**	**7.48**	5.115
$C_{M_{m_\alpha}}$	-0.5402	-0.5402	-0.5402	-0.5402	-0.5402
C_{L_q}	5.9649	5.9649	5.9649	5.9649	5.9649
$C_{M_{mq}}$	-6.9263	-6.9263	-6.9263	**-8.6516**	**-16.169**

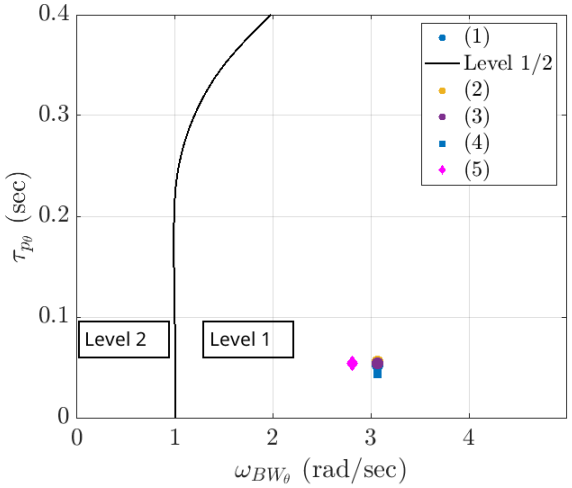

[1] The applied levels are derived from helicopter standards and may require revision to align with eVTOL-specific characteristics.

Figure 24. Bandwidth and phase delay variability due to the uncertainty of aerodynamic parameters.[1]

The parameters selected from the previous MOAT and VBD analyses are C_{L_0}, C_{L_α}, and C_{Mm_q} (see Table 5). Figure 24 shows the bandwidth and phase delay results for different aerodynamic data sets. Similarly to Attitude Quickness, Bandwidth and Phase Delay are not significantly sensitive to aerodynamic parameters. Changes in C_{L_0} and $C_{L\alpha}$ (Cases 2 and 3) result in a minimal increase in τ_d, while C_{Mm_q} causes a decrease in τ_d of approximately 17%. However, it is worth noting that the phase delay is generally very low because the model does not include a delay in propeller response, considering only the intrinsic delay of the control system.

After significantly modifying the derivative C_{Mm_q} to cross-check with previous computations, a dependency of ω_{BW} also becomes evident.

CONCLUSIONS

The applied SA analysis demonstrated that a valid framework can be built coupling the FSM with an external statistical tool, such as Dakota. The chosen methods , MOAT and emulator-based VDB, show satisfactory agreement in identifying the most influential factors, with a relatively small number of simulations.

Concerning Attitude Quickness, the SA showed that most of pHQ variance is to be ascribed to changes in the quickness parameter $q_{\text{pk}}/\Delta\theta_{\text{pk}}$: mass, inertia, and rotor-related factors play a primary role, while aerodynamics contributes to the problem only secondarily through C_{L_0} and C_{L_α}. Minimum attitude change $\Delta\theta_{min}$ depends on a much wider set of factors, among which aerodynamics coefficients and stability derivatives prevail, but shows little to no variability. A possible cause for this behavior can be sought in the limited pitch angles , constrained by the applied linear aerodynamic model, or by the intrinsic robustness of this pHQ on FSM aerodynamic parameters. The aerodynamic analysis that follows the SA, confirms that the Attitude Quickness is relatively insensitive to aerodynamic parameter variations, under low-speed and small-amplitude conditions.

Dynamic stability is situated at the boundary between Levels 1 and 2, with Level 2 values mainly caused by the coupled $M - \tau_{\text{d}}$ effect on ζ. Dynamic Stability exhibits higher sensitivity to aerodynamic parameters, particularly C_{L_0} and $C_{M_{mq}}$, in comparison to Attitude Quickness. Variations in the lift coefficient C_{L_0} have a pronounced impact on damping, bringing the pHQ closer to Level 1 under the analyzed conditions. Failing to account for the reduction in C_{L_0} caused by propeller wake interference may lead to an overestimation of stability.

Bandwidth analysis revealed that for the SA, the linearization approach can satisfactorily substitute the application of an automated sweep to the non-linear FSM, to significantly reduce the computational effort. However, high-amplitude commands should be applied too, to explore possible discrepancies arising further from the linearization point. The MC analysis indicated that most of the variability is to be attributed to $\omega_{BW_{\text{phase}}}$, which is mostly sensitive to M, K_T, I_y and C_{Mmq}. In the aerodynamic analysis, bandwidth and phase delay were

found to be rather non-sensible to aerodynamic parameters alone, with C_{Mmq} having the highest impact on bandwidth, which confirms the SA results.

Overall, among aerodynamic parameters, C_{L_0} and $C_{M_{mq}}$ have the most significant impact on the analyzed pHQs. In order to better characterize their effect, an aerodynamics-only SA could be conducted, using the coupled Dakota/FSM approach.

Having identified the predominant uncertain factors and building on the preliminary SA results, a deeper characterization of inputs' ranges and probability distributions may be considered, to resize the effect of mass, inertia, and rotor-related parameters (which in some cases may absorb the majority of output variance, thus overshadowing aerodynamics) and to account for possible range-dependent behaviours or nonlinearities which may occur beyond the intervals' limits employed in this study. Similarly, pHQ manoeuvres could be executed at different V_{lon}, as to investigate the dependency of aerodynamics on the test velocity.

Given the width of Dakota capabilities, different MOAT settings could be studied, as well as different meta-modelling techniques may be introduced in the SA framework to compute, for example, second-order interactions between parameters.

The aerodynamic analysis using DUST simulations demonstrated that the trend of the lift dynamic derivative due to pitching, $C_{Lq} + C_{L\dot{\alpha}}$, corresponds to the trend predicted by the Theodorsen model. Therefore, the methodology for obtaining stability derivatives due to pitch rate is proven to be correct, but the dependency on the reduced frequency should be accounted for when building the FSM, or at least in the later stage of RCbS, during uncertainty analysis. To obtain pure C_{Lq} and C_{Mmq} derivatives, a phugoid maneuver should be simulated in DUST.

The research presented in this paper demonstrates how to perform a robust and automated sensitivity analysis, as an essential component of uncertainty analysis, and how to propagate model input uncertainties onto the final pHQ metrics. This activity supports the model user in gaining a deeper understanding of the uncertainty in FSM predictions, thereby enabling correct decisions within the certification process and building model credibility with the authority.

Author contact:
Agata Rylko - agata.rylko@polimi.it
Lorenzo Favaro - lorenzo.favaro@mail.polimi.it
Giuseppe Quaranta - giuseppe.quaranta@polimi.it

ACKNOWLEDGMENTS

The work in this study done by Agata Rylko was carried out within the 38th cycle of doctoral study in aerospace engineering, in the research field "Policymaking for Urban Air Mobility acceptance" and received funding from PIANO NAZIONALE DI RIPRESA E RESILIENZA (PNRR). The work in this study done by Giuseppe Quaranta was carried out within MOST -– Sustainable Mobility National Research Center and received funding from the European Union Next-Generation EU (PIANO NAZIONALE DI RIPRESA E RESILIENZA (PNRR) – MISSIONE 4 COMPONENTE 2, INVESTIMENTO 1.4 – D.D. 1033 17/06/2022, CN00000023). This manuscript reflects only the authors' views and opinions, neither the European Union nor the European Commission can be considered responsible for them.

REFERENCES

1. Anon., *Third Publication of Means of Compliance with Special Condition VTOL, MOC-3 SC-VTOL Issue 2*, Cologne, Germany, EASA, 2023.

2. Anon., *ED-295, Guidance on VTOL Flight Control Handling Qualities Verification*, EUROCAE, 2024.

3. Anon., *Proposed Revisions to Aeronautical Design Standard – 33E (ADS-33E-PRF) Toward ADS-33F-PRF*, U.S. Army Combat Capabilities Development Command, Redstone Arsenal, AL, September 2019.

4. Lu, L., van't Hoff, S., Padfield, G., Podzus, P., Quaranta, G., and White, M., *Rotorcraft Certification by Simulation and Analysis; an Introduction to the Principles and Practices*, Springer, to be published, 2023.

5. Rylko, A., van't Hoff, S., Lu, L., Padfield, G., Podzus, P., White, M., and Quaranta, G., "Rotorcraft Flight Simulation to Support Aircraft Certification: A Review of the State of the Art with an Eye to Future Applications," 49th European Rotorcraft Forum, Bückeberg, Germany, September 2023.

6. Rylko, A., Quaranta, G., and M., L., "Aerodynamic Model Development and Fidelity Assessment for eVTOL Predicted Handling Qualities," 50th European Rotorcraft Forum, Marseille, France, September 2024.

7. Battaini, N., *Design and dynamic modeling of a VTOL UAV*, Master's thesis, Politecnico di Milano, Italy, 2019.

8. Martinelli, E., *Modelling, control, integration and testing of an eVTOL drone*, Master's thesis, Politecnico di Milano, Italy, 2022.

9. Martello, N. C., *Modelling and integration of an eVTOL UAV*, Master's thesis, Master Thesis, Politecnico di Milano, Italy, 2021.

10. Marchesi, M., *Structural redesign, simulation, control, and state estimation of an eVTOL UAV*, Master's thesis, Politecnico di Milano, Italy, 2024.

11. Campolongo, F., Cariboni, J., and Saltelli, A., "An effective screening design for sensitivity analysis of large models," *Environmental Modelling & Software*, Vol. 22, (10), 2007, pp. 1509–1518.

12. Saltelli, A., Tarantola, S., Campolongo, F., and Ratto, M., *Sensitivity Analysis in Practice. A Guide to Assessing Scientific Models*, Wiley, 2004.

13. Saltelli, A., Ratto, M., Andres, T., Campolongo, F., Cariboni, J., Gatelli, D., Saisana, M., and Tarantola, S., *Global Sensitivity Analysis*, Wiley, 2008.

14. Dalbey, K., Eldred, M., Geraci, G., Jakeman, J., Maupin, K., Monschke, J., Seidl, D., Swiler, L., Tran, A., Menhorn, F., and Zeng, X., *Dakota, A Multilevel Parallel Object-Oriented Framework for Design Optimization, Parameter Estimation, Uncertainty Quantification, and Sensitivity Analysis: Version 6.14 Theory Manual*, Sandia National Laboratories, Albuquerque, NM, 2021.

15. Campolongo, F., and Saltelli, A., "Sensitivity analysis of an environmental model: an application of different analysis methods," *Reliability Engineering & System Safety*, Vol. 57, (1), 1997, pp. 49–69.

16. Menberg, K., Heo, Y., and Choudhary, R., "Sensitivity analysis methods for building energy models: Comparing computational costs and extractable information," *Energy and Buildings*, Vol. 133, 2016, pp. 433–445. DOI: 10.1016/j.enbuild.2016.10.005.

17. Gan, Y., Duan, Q., Gong, W., Tong, C., Sun, Y., Chu, W., Ye, A., Miao, C., and Di, Z., "A comprehensive evaluation of various sensitivity analysis methods: A case study with a hydrological model," *Environmental Modelling & Software*, Vol. 51, 2013, pp. 269–285. DOI: 10.1016/j.envsoft.2013.09.031.

18. Nabi, H., de Visser, C., Pavel, M., and Quaranta, G., "A quasi-Linear Parameter Varying (qLPV) Approach for Tiltrotor Conversion Modeling and Control Synthesis," Vertical Flight Society 75th Annual Forum & Technology Display Proceedings, Philadelphia, PA, May 13–16, 2019.

19. Marcos, A., and Balas, G., "Development of LinearParameter-Varying Models for Aircraft," *Journal of Guidance, Control and Dynamics*, Vol. 27, 2004, pp. 218–228. DOI: 10.2514/1.9165.

20. Adams, B., Bohnhoff, W., Dalbey, K., Ebeida, M., Eddy, J., Eldred, M., Hooper, R., Hough, P., Hu, K., Jakeman, J., Khalil, M., Maupin, K., Monschke, J., Ridgway, E., Rushdi, A., Seidl, D., Stephens, J., Swiler, L., Tran, A., and Winokur, J., *Dakota, A Multilevel Parallel Object-Oriented Framework for Design Optimization, Parameter Estimation, Uncertainty Quantification, and Sensitivity Analysis: Version 6.16 User's Manual*, Sandia National Laboratories, Albuquerque, NM, 2022.

21. Anon., *Dakota Sensitivity Analysis and Uncertainty Quantification, with Examples*, Sandia National Laboratories, 2014.

22. Anon., *Dakota Software Training, Surrogate Models*, Sandia National Laboratories, 2016.

23. Cocco, A., Saetti, U., and Savino, A., "Aeroelastic Load Evaluation During Tiltrotor Transition Using a Comprehensive Mid-Fidelity Approach," 50th European Rotorcraft Forum, Marseille, France, September 2024.

24. Granata, D., Savino, A., and Zanotti, A., "Numerical Evaluation of Aircraft Aerodynamic Static and Dynamic Stability Derivatives by a Mid-Fidelity Approach," *Aerospace*, Vol. 11, (3), 2024. DOI: 10.3390/aerospace11030213.

25. Granata, D., Savino, A., and Zanotti, A., "Numerical Calculation of a Tiltrotor Aircraft Aerodynamic Stability Derivatives," 50th European Rotorcraft Forum, Marseille, France, September 2024.

26. Mamino, M., *Comparison of Uncertainty Quantification and Validation Methodologies on a Civil Tiltrotor Flight Simulation Model*, Master's thesis, Politecnico di Milano, Italy, 2023.

27. Pavel, M., and Padfielf, G., "Progress in the development of complementary handling and loading metrics for ADS-33 manoeuvres," American Helicopter Society 59th Annual Forum Proceedings, Phoenix, AZ, May 6–8, 2003.

28. Anon., *Test Guide for ADS-33E-PRF*, U.S. Army Research, Development, and Engineering Command, Moffet Field, CA, July 2008.

29. Rodden, W. P., and Giesing, J. P., "Application of oscillatory aerodynamic theory to estimation of dynamic stability derivatives," *Journal of Aircraft*, Vol. 7, (3), 1970, pp. 272–275.